mentum. To obtain a treatment of radiation forces on medium inhomogeneities it was necessary in the course of this investigation to modify certain normally accepted notions which stood in the way of a coherent development of the subject matter. They were:

(1) The commonly hidden assumption of homogeneity in the derivation of energy-momentum relations.

(2) The too-specialized definition of the wave momentum of radiation in terms of $c$.

(3) The impermissible imposition of a strict symmetry requirement on the energy-momentum tensor.

It should also be clear from the previous discussion that a considerable amount of detail and physical subtlety can be concealed in the transformation behavior of physical fields

It should be stressed that the present treatment of radiation forces is only a minor step towards a more coordinated description of energy-momentum relations. Further and deeper-going modifications are necessary.[10]

In this connection it is important to note that many physical distinctions developed in this article vanish under the customary substitution $ict=x_0$. The latter changes the indefinite metric into a definite metric thus obscuring how the physical identification of fields depends on the co- and contra-gradient behavior of transformation.

Finally it should be remarked that the description of nonuniformity requires the existence of a reference of uniformity. The use of local Cartesian frames is thus important for singling out the results of true physical inhomogeneities in the expression $\partial_{(\lambda)}\mathfrak{L}$ for the radiation force density.

[10] The physical meaning of the formal symmetrization procedures for the energy-momentum tensor for instance is a future topic to be considered.

PHYSICAL REVIEW VOLUME 133, NUMBER 3A 3 FEBRUARY 1964

# Zeeman and Coherence Effects in the He-Ne Laser*

W. CULSHAW† AND J. KANNELAUD†
*Research Laboratories, Lockheed Missiles and Space Company, Palo Alto, California*
(Received 7 August 1963)

An account is given of further investigations of the Zeeman effect on the He-Ne laser transition at $\lambda=1.153\,\mu$, using both planar- and confocal-type resonators. For Zeeman level separations larger than the natural linewidths, the specific polarizations of the Zeeman transitions for the appropriate geometry are observed in the planar laser. Low-frequency splittings of axial resonances associated with anomalous dispersion effects occur under these conditions, the polarizations of these being linear, or circular, and orthogonal. At values of magnetic field such that the Zeeman levels overlap, coherence effects in the induced radiation are made evident by the disappearance of such low-frequency beats and by changes in these polarizations. This is considered using the theory of the depolarization of resonance radiation by magnetic fields, and also using time-dependent perturbation methods. For a symmetrical location of the axial resonance within the Doppler-broadened line, linear polarization is predicted for axial magnetic fields such that the states overlap, and some experimental verification is given. Related effects occur in the confocal laser where the Brewster angle windows determine the polarization. Here oscillations may be inhibited, or modulated by axial magnetic fields. Dips in the power output of this laser occur at smaller magnetic fields and are presently associated with interference effects when the Zeeman levels overlap. Some indications are given of coupling effects at Zeeman separations corresponding to the frequency interval between axial resonances.

## 1. INTRODUCTION

INVESTIGATIONS of the Zeeman effect have played a dominant role in the development of the quantum mechanical interpretation of atomic spectra. Wood and Ellett[1] in their pioneering work on the polarization of resonance radiation, mention the large depolarizing effects of small magnetic fields on the resonance radiation of mercury. The largest effect was obtained when the atoms were excited by incident $\pi$ mode radiation and the polarization of the resonance radiation was observed using the $\sigma$ transitions. For zero magnetic field the observed polarization was 90%, while for a field of 2 Oe the polarization was less than 1%. The polarization of the resonance radiation is thus linear, and in the same direction as that of the incident radiation for zero magnetic field, but decreases continuously with increasing magnetic field, becoming elliptical with a rotation of the plane of maximum polarization. Similar variations in the polarization occur for other orientations of the magnetic field and incident polarization, the phenomena now being called the Hanle effect,[2] who made a thorough investigation of it.

† Formerly at the General Telephone and Electronics Labs, Inc., Palo Alto, California.

* Research on report is supported by the Independent Research Program of Lockheed Missiles & Space Company.

[1] R. W. Wood and A. Ellett, Phys. Rev. 24, 243 (1924).

[2] A. C. G. Mitchell and M. W. Zemansky, *Resonance Radiation and Excited Atoms* (Cambridge University Press, New York, 1934), pp. 258–317.

Similar effects occurred with the other atoms but these differed greatly in degree. For example, with sodium there was practically no polarization at zero magnetic field, and to produce the effects found in mercury at fields of a few oersteds, required fields of some hundred oersteds.

Theoretical expressions based on the classical Zeeman effect were derived by Eldridge[3] and Breit[4] by assuming the atomic radiator to act as a damped vibrating electric dipole processing about the direction of the magnetic field, and absorbing and emitting only linear polarization. This treatment explained the polarization phenomena observed in the mercury resonance line, which has a normal Zeeman effect apart from a $g$ factor of $\frac{3}{2}$, but was completely unable to explain the results obtained on the polarization of the resonance radiation of sodium. Such work did, however, relate the depolarizing effects to what is now termed the $g$ factor and to the lifetime of the excited states.

Hanle[5] was the first to apply the quantum theory to the phenomena by considering the specific polarizations involved in the various Zeeman transitions of the line in question. Later Weisskopf[6] derived expressions for the polarization and rotation of the plane of maximum polarization in a magnetic field on the basis of Dirac's quantum mechanical treatment of an atom in a radiation field. This work was extended by Breit[7] to the case of hyperfine structure in a remarkably thorough and deep treatment of the quantum theory of dispersion. Such depolarization effects, or departures from the specific polarizations associated with the Zeeman transitions, occur when the Zeeman splitting is smaller than the natural linewidths due to the radiative damping or lifetimes of the excited states. Coherent excitation and spontaneous emission processes then occur, leading to interference effects between the radiations from such overlapping states.

These results were used by Franken[8] to discuss the results obtained in the level crossing experiments on helium.[9] Here crossings occur at specific values of magnetic field between certain of the magnetic sublevels of the $^3P_1$ and $^3P_2$ states, whence interference effects occur leading to changes in the intensity of the 10 830 Å line of helium, provided the matrix elements involved between the levels which cross, and one of the $^3S_1$, sublevels have finite values for the incident and radiated polarizations. The same considerations apply also to the double resonance work of Brossel and Bitter,[10] Dodd and Series,[11] and Barrat.[12] Here the coherence between the separated Zeeman levels of the resonance line is imparted by an rf magnetic field oscillating in the plane perpendicular to the dc magnetic field. The values of the field for resonance and modulation of the resonance fluorescence depend on the orientation of the incident polarization, or on the coherence properties between the states imparted by this and the rf perturbation. In particular for the resonance line of mercury, resonances due to the rf perturbation can occur at fields $\frac{1}{2}H_0$, $H_0$, $\frac{3}{2}H_0$, $2H_0$, and $3H_0$, together with possible modulation of the intensity at frequencies $\omega_0$, $2\omega_0$, $3\omega_0$, and $4\omega_0$, where $\omega_0$ is the rf frequency, and $H_0$ is the field for which $\omega_0$ is the Larmor frequency.

We may expect similar effects to occur in gas lasers, with modifications due to the pronounced effects of induced emission and the very high monochromaticity of the radiation. Although the Zeeman splitting in such investigations is considerably less than the Doppler widths of the transitions involved in resonance fluorescent, or in the gas laser, the polarization characteristics of the Zeeman transitions are clearly defined, provided the separation is greater than the natural linewidths, and hence represent a powerful method of investigation. In the gas laser simultaneous oscillations in modes with orthogonal circular and linear polarizations may be expected, depending on the orientation of the magnetic fields. These will be apparent from the appearance of beat frequencies in the laser output, and such beats will be sensitive to the orientation of a Nicol prism, or other analyzer, in the output beam to the photomultiplier. Some work on such Zeeman effects in gas lasers has already been published.[13–15] In this paper we present results of further investigations on both the planar and confocal types of gas laser, together with some interesting results on coherence effects between the magnetic sublevels, which appear in such lasers at values of magnetic field where the natural linewidths of the levels overlap. This results in laser transitions involving a coherent mixture of such states, and in departures from the specific polarizations such as circular associated with an axial magnetic field. Such effects are analogous to those discussed above for the case of spontaneous emission. They are, however, of some interest in accounting for the behavior of gas lasers as regards polarization and frequency content, also for studies involving coherence effects, lifetimes, and $g$ factors of the states involved in the laser transitions.

[3] J. A. Eldridge, Phys. Rev. **24**, 234 (1924).
[4] G. Breit, J. Opt. Soc. Am. **10**, 439 (1925).
[5] W. Hanle, Z. Physik **30**, 93 (1924).
[6] V. Weisskopf, Ann. Physik **9**, 23 (1931).
[7] G. Breit, Rev. Mod. Phys. **5**, 91 (1933).
[8] P. A. Franken, Phys. Rev. **121**, 508 (1961).
[9] F. D. Colegrove, P. A. Franken, R. R. Lewis, and R. H. Sands, Phys. Rev. Letters **3**, 420 (1959).
[10] J. Brossel and F. Bitter, Phys. Rev. **86**, 308 (1952).
[11] J. N. Dodd, W. N. Fox, G. W. Series, and M. J. Taylor, Proc. Phys. Soc. (London) **74**, 789 (1959); J. N. Dodd and G. W. Series, Proc. Roy. Soc. (London) **A263**, 353 (1961).
[12] J. P. Barrat, Proc. Roy. Soc. (London) **A263**, 371 (1961).
[13] W. Culshaw and J. Kannelaud, Phys. Rev. **126**, 1747 (1962).
[14] H. Statz, R. Paananen, and G. F. Koster, J. Appl. Phys. **33**, 2319 (1962); R. Paananen, C. L. Tang, and H. Statz, Proc. Inst. Elect. and Electronics Engrs. **51**, 63 (1963).
[15] W. Culshaw and J. Kannelaud, Third International Symposium on Quantum Electronics, Paris, France, 1963 (unpublished).

## 2. ZEEMAN EFFECT CONSIDERATIONS

Breit[7] discusses the polarization of the resonance radiation due to transitions between the magnetic sublevels $\mu$ and $m$ of the upper and lower states respectively, of a single scattering atom, and derives an expression for the probability amplitude of the scattering atom being in the state $m$ there being a photon of the type $g$ emitted. Summing over the states $\mu$, the expression may be written as

$$c_g=(i\Gamma_1)^{-1}\sum_{\mu}\frac{f_{\mu m}g_{m\mu}\exp\{-2\pi i(\nu_g-\nu_m)\}}{\nu_g-\nu(\mu,m)+i\Gamma}, \quad (1)$$

with the condition that $\Gamma_1$ the decay constant of the source atoms is very large. Some further discussion of this point has been given by Franken,[8] the formula remaining valid for finite $\Gamma_1$ under the condition of weak excitation by the source atoms. In Eq. (1) $f_{\mu m}=(\mu|\mathbf{f}\cdot\mathbf{r}|m)$ is the electric dipole matrix element for excitation of the scattering atom by incident photons of polarization $\mathbf{f}$. Similarly, $g_{m\mu}=(m|\mathbf{g}\cdot\mathbf{r}|\mu)$ is the matrix element corresponding to the emission of photons of polarization $\mathbf{g}$. The decay constant $\Gamma=(4\pi\tau)^{-1}$, $\tau$ is the lifetime of the $\mu$ levels, $\nu(\mu,m)$ is the frequency separation between levels $\mu$ and $m$, and $\nu_g$ is the frequency of the emitted photon, which is assumed to be in the region of $\nu(\mu,m)$. The probability, or rate of emission of photons of type $g$, is then given by

$$|c_g|^2=K\sum_{\mu\mu'}\frac{f_{\mu m}f_{m\mu'}g_{\mu' m}g_{m\mu}}{[\nu_g-\nu(\mu,m)+i\Gamma][\nu_g-\nu(\mu',m)-i\Gamma]}, \quad (2)$$

where $K$ is a constant. We note that in order for interference terms to occur in the expansion, the excitation and decay of the states in question must occur as a coherent process. When the Zeeman levels $\mu$ are separated by more than the natural linewidth $2\Gamma$, coherent emission of photons of type $g$ at the frequency $\nu_g$ is no longer possible, the terms representing the interference of probability amplitudes become small, and the transition then occurs between separate states.

Under conditions of low excitation or during the build up of oscillations, Eq. (2) is applicable to the gas laser and indicates that departures from the specific polarizations associated with the Zeeman transitions, together with possible intensity changes, will occur when the Zeeman levels are separated by less than the natural linewidths of the transitions. Such effects will occur only when a given atom can be excited as a coherent mixture of its eigenstates, and also can be stimulated to emit as a coherent mixture of such states. In the He–Ne gas laser the excitation of the Ne atoms occurs through collisions of the second kind with the metastable helium atoms. We shall assume that such collisions result in the coherent excitation of the magnetic sublevels when these overlap within their natural linewidths. The resulting excitation will also be assumed isotropic. There may be some weighting factors in the population probabilities of the magnetic sublevels during such collisions, but the above seems a reasonable assumption at the present time. This renders the excitation process, analogous to the terms $f_{m\mu}f_{m\mu'}$ in Eq. (2), equal for all $\mu$ and $m$. It is clear then that for the planar laser, which ideally is isotropic as regards polarization, changes in the polarization of the laser radiation should occur when dc magnetic fields are applied, and in particular when the Zeeman separation is smaller than the natural linewidth of the laser transition. Similar effects will occur in the confocal or Brewster angle laser, and will be mentioned later. It is of course, necessary to apply the methods of time-dependent perturbation theory to this problem in view of the relatively large electromagnetic fields in the laser, this will be done in a later section, and a result analogous to Eq. (2) there derived. When the Zeeman transitions are separated beyond the natural widths of the $\mu$ and $m$ levels, the specific polarizations associated with the transitions $\Delta M=\pm1, 0$ for the given orientation of the magnetic field and laser axis will be obtained. Some modification of Eq. (2) is necessary in the case of the laser transitions in He–Ne since both the states involved have finite lifetimes, in this case $\Gamma$ in this equation would represent the sum of the decay constants.

Breit[7] then integrates Eq. (2) over all possible values of $\nu_g$ corresponding to the summation of the spontaneously emitted radiation over all possible transitions and linewidths. This process differs from that applicable to the laser where we must deal with the induced emission due to the highly monochromatic radiation involved, but the result brings out some points of interest to the present discussion. This gives the rate of emission of photons of type $g$, or the intensity with polarization $\mathbf{g}$ as

$$I_g=K\sum_{\mu\mu' mm'}\frac{f_{\mu m}f_{m\mu'}g_{\mu' m'}g_{m'\mu}}{1-2\pi i\tau\nu(\mu,\mu')}. \quad (3)$$

From which we see that interference terms will arise in the summation of intensities when $2\pi\tau\nu(\mu,\mu')<1$, and that these will become small when this factor is greater than unity, the effective transitions then being those between pure states. The intensity of radiation with polarization $\mathbf{g}$ due to any incident polarization $\mathbf{f}$ may now be determined from Eq. (3). Applying this to the geometry concerned in the Hanle effect as shown in Fig. 1 the depolarization of resonance radiation is given by

$$P=\frac{I_x-I_y}{I_x+I_y}=\frac{P_0}{1+(\tau geH/mc)^2} \quad (4)$$

for the case of no hyperfine structure. The rotation of the plane of maximum polarization is also given by

$$\tan 2\theta=\tau geH/mc. \quad (5)$$

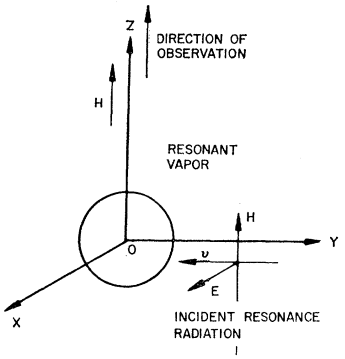


FIG. 1. Geometry for depolarization of resonance radiation (Hanle effect).

These formulas were initially derived by Weisskopf,[6] and later extended by Breit[7] to cover the case of hyperfine structure. $P_0$ is the polarization in zero magnetic field, and may be deduced from the matrix elements, or by applying the principle of spectroscopic stability in the form of Heisenberg's rule,[16] which states that the polarization in zero magnetic field is the same as that obtained by applying a strong magnetic field in the direction of the incident electric vector. Applied to the resonance line of mercury, the polarization is linear at zero magnetic field, then becomes elliptical, and finally unpolarized as the magnetic field is increased such that the normal independent circular polarized transitions occur between pure state. Similar results, again with differences due to the monochromatic radiation involved, are found in the effects of axial magnetic fields on the gas laser.

The basic polarizations involved in the Zeeman transitions are shown in Fig. 2 with the magnetic field along the $z$ axis. The electric dipole transitions involved in the He–Ne laser are those from an upper state of total angular momentum $j-1$ to a lower state $j$, and the matrix elements are thus given by[17]

$$(\alpha jm|\mathbf{r}|\alpha' j-1 m\pm 1) = \pm(\alpha j:r:\alpha' j-1)\tfrac{1}{2}[(j\mp m)(j\mp m-1)]^{1/2}(\mathbf{i}\pm i\mathbf{j}), \quad (6)$$
$$(\alpha jm|\mathbf{r}|\alpha' j-1 m) = (\alpha j:r:\alpha' j-1)(j^2-m^2)^{1/2}\mathbf{k}.$$

The direction of rotation of the electric vector for the circularly polarized transitions may be deduced from Eq. (6). For $\Delta m=-1$ it rotates from the $x$ axis to the $y$ axis, or is left circularly polarized as viewed from the positive $z$ direction; for $\Delta m=+1$ it rotates from the $y$ axis to the $x$ axis or is right circularly polarized. With a planar laser orientated with its axis along the $z$ axis, the laser radiation will contain oscillations of both right- and left-handed circular polarization, provided the Zeeman separation of the states, given by $\Delta\omega = geH/2mc$, is greater than the natural linewidth $1/\tau$. With the laser axis along the $x$ or $y$ axes the observed polarizations will be linear and orthogonal for similar values of magnetic field. Laser oscillations thus build up separately in the distinct polarizations, or different photon types available in the Zeeman transitions. The polarizations possible with the laser axis oriented at angles $\theta$ and $\phi$ in polar coordinates, may be deduced from the form of the radiation patterns of the dipole moments involved.[18] Thus, for $\Delta m=0$, this is of the form $P\mathbf{k}$, and produces a dipole field with a $\sin\theta$ variation. The other dipole terms for $\Delta m=\pm 1$, viz., $\mathbf{i}\pm i\mathbf{j}$, give radiation fields

$$\mathbf{E}\propto(\boldsymbol{\theta}_0\cos\theta\pm i\boldsymbol{\phi}_0)\exp(\pm i\phi),$$

where $\boldsymbol{\theta}_0$ and $\boldsymbol{\phi}_0$ are unit vectors. Thus, elliptical polarization will be observed in the laser output as the angle $\theta$ is increased. For orientations around $\theta=0$, however, the polarizations will be as specified above, and will be relatively insensitive to any slight misalignment about this position. Any appearance of elliptical polarization at low values of magnetic field may thus be ascribed to coherence effects.

Figure 3 shows the Zeeman splitting for the strongest transitions in the He–Ne laser. These are in Paschen notation, the $2s_2\rightarrow 2p_4$ $(J=1\rightarrow 2)$ transition at $\lambda=1.153\mu$,[19] the $3s_2\rightarrow 2p_4$ $(J=1\rightarrow 2)$ transition at $\lambda=0.6328\mu$,[20] and the $3s_2\rightarrow 3p_4$ $(J=1\rightarrow 2)$ transition at $\lambda=3.39\mu$.[21] Those values of the $g$ factor which have been measured are also indicated in the figure. The coupling of the angular momentum in neon approximates the $LS$ type for the electron configuration $2p^5 3s$, and approximates the $jj$ type for the higher electron configurations $2p^5 ns$, and $2p^5 np$. For the $2p^5 4s$ ($2s$ Paschen) and $2p^5 3p$ ($2p$) levels the coupling is of an intermediate nature. Measurements give $g=1.301$ for the $2p_4$ level whereas computations give 1.5, 7/6, and 4/3 for $LS$, $jj$- and Racah-type[22] $jl$ coupling, respec-

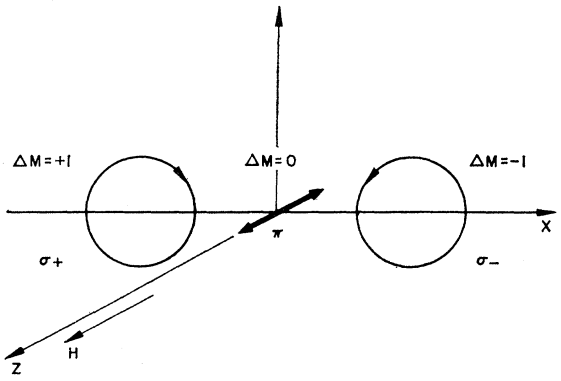


FIG. 2. Normal Zeeman effect showing the basic photon polarization involved.

[16] W. Heisenberg, Z. Physik **31**, 617 (1926).
[17] E. U. Condon and G. H. Shortley, *The Theory and Atomic Spectra* (Cambridge University Press, New York, 1935), p. 63.
[18] E. U. Condon and G. H. Shortley, *The Theory and Atomic Spectra* (Cambridge University Press, New York, 1935), pp. 90–92.
[19] A. Javan, W. R. Bennett, Jr., and D. R. Heriott, Phys. Rev. Letters **6**, 106 (1961).
[20] A. D. White and J. D. Rigden, Proc. IRE **50**, 1697 (1962).
[21] A. L. Bloom, W. E. Bell, and R. C. Rempel, Appl. Opt. **2**, 317 (1963).
[22] G. Racah, Phys. Rev. **61**, 537 (1942).

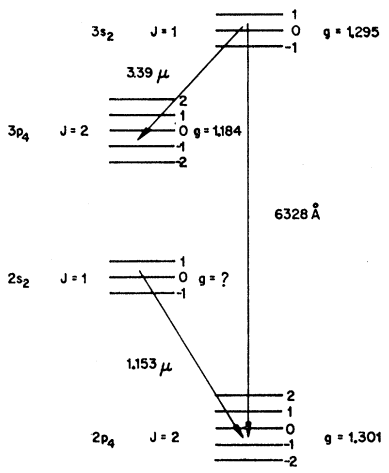


FIG. 3. Zeeman splitting of the various transitions in He—Ne lasers.

tively. Similarly for the $2s_2$ level, computations give the values 1 ($LS$), 4/3 ($jj$), and 4/3 (Racah), no measured value being available. The coupling here is certainly not $LS$, and the computations indicate that $g=4/3$ approximately for the $2s_2$ level. A reasonable assumption is that the $g$ values of the upper $2s_2$ and lower $2p_4$ levels of the laser transition at $\lambda=1.153\mu$ are approximately identical. Measurements give $g=1.295$ for the $3s_2$ level of the $2p^5 3s$ electron configuration, while computed values are 4/3 for both $jj$ and $jl$ couplings. For the $3p_4$ level of the $3.39\mu$ laser transition measurements give $g=1.184$, whereas computed values are 1.5 ($LS$), 7/6 ($jj$), and 4/3 ($jl$). Such considerations are important for considerations of laser operation, particularly at the higher values of magnetic field, since with different $g$ values for the upper and lower states the various Zeeman transitions possess different frequencies, and will separate leading to variations of the over-all gain from such transitions. This is also important in the application of the laser to the accurate determinations of $g$ factors.

From the preceding considerations we can infer that laser oscillations will occur with photons of specific types corresponding to the $\Delta m=0, \pm 1$ transitions, and providing the Zeeman levels are separated beyond the natural linewidth all transitions corresponding to say $\Delta m=+1$ may be summed, and a resultant transition or gain curve determined by the matrix elements $\sum_m(\alpha jm|x+iy|\alpha' j-1m-1)$ may be deduced. Similarly for the transitions $\Delta m=-1$ or 0. Each transition thus adds its contribution to the over-all gain independently, although of course all transitions are rendered phase coherent by the laser oscillation in the specific polarization. As already pointed out the situation is different when the Zeeman levels overlap, since interference effects between the various transitions then occur. Figures 4 and 5 show such gain curves computed for the $1.153\mu$ laser transition for axial and transverse fields of 30 Oe, and an assumed $g$ value of 1.3 for the upper and lower levels.

So far we have considered the neon atoms to have a fixed velocity; actually conditions within the discharge lead to a Doppler distribution of frequencies corresponding to a temperature of the neon atoms of some 400°K, which results in a Doppler width of 800 Mc/sec. The shape of the gain curve over this frequency range is due to the superposition of a large number of Lorentzian lines due to transitions in atoms with differing velocities. Using Bennett's work[23] the shape

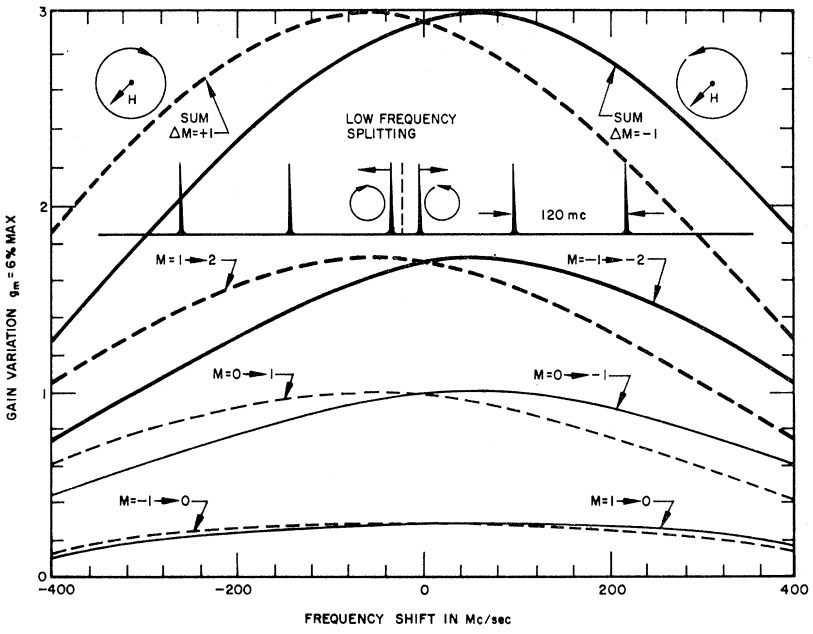


FIG. 4. Zeeman splitting of the $1.153\mu$ laser transition for an axial magnetic field of 30 Oe. $g$ values of upper and lower states taken as 1.3. Low-frequency splitting of axial resonances also shown.

[23] W. R. Bennett, Jr., Phys. Rev. **126**, 580 (1962).

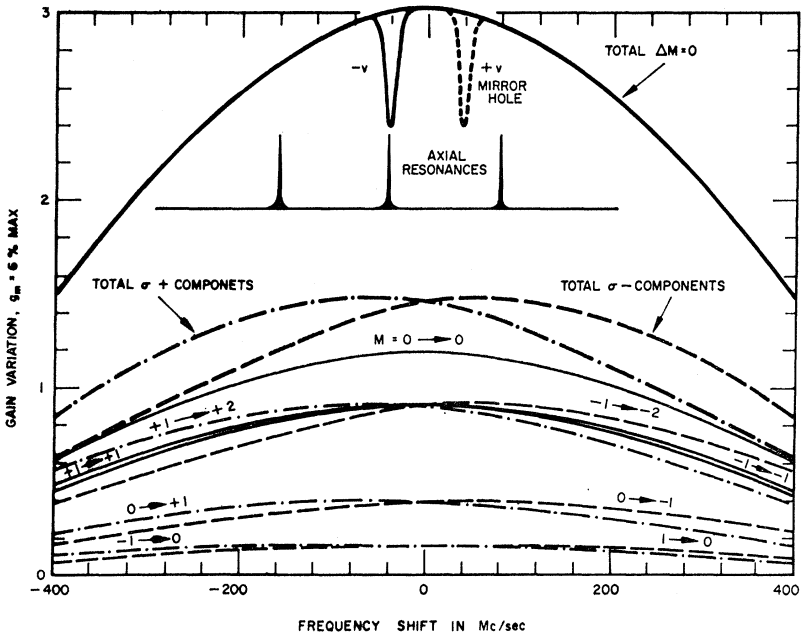


FIG. 5. Zeeman splitting of the 1.153 $\mu$ laser transition for a transverse field of 30 Oe. Additional resonances with atoms of opposite velocities are also shown (see Ref. 27).

of this is taken as Gaussian determined by the equation

$$g(\nu)=g_m \exp\left[-\left(\frac{\nu_m-\nu}{0.6\Delta\nu_m}\right)^2\right] \tag{7}$$

with $0.6\Delta\nu_m=500$ Mc/sec. Resonances due to the axial modes of the planar resonator, given by $2\epsilon d=n\lambda$, $\epsilon$ being the dielectric constant of the laser medium, and $d$ the reflector spacing, $\approx 1m$, are also indicated. Such resonance frequencies determine the laser oscillation frequency to a high degree. It is clear, however, that provided there is no overlapping within a natural linewidth, for an axial magnetic field two distinct photon types of opposite circular polarization are available for the given axial resonance. Above threshold then a low-frequency splitting will occur giving rise to two oscillations, with orthogonal circular polarizations instead of the single axial resonance. Such a splitting may be deduced from a consideration of the anomalous dispersion for the case of stimulated emission whereby the cavity frequency, due to the changes in the dielectric constant, is shifted towards the centers of the respective lines. It may also be considered in this case as due to a Faraday rotation, the dielectric constant of the laser medium now being different for the right- and left-handed circular polarizations.

Such pulling effects have been discussed by Bennett[23] for the degenerate case, with reference to pulling effects between different axial modes of the resonator. His treatment, based on phase-shift considerations in the resonator, gives the frequency of the $j$th cavity resonance as

$$\tilde{\nu}_j=\nu_j-\frac{\Delta\nu_c}{f}\Delta\phi_m(\nu_j)-\frac{\Delta\nu_c}{4}\sum_{i\neq j}\left(\frac{g(\nu_i)}{f}-1\right)\left(\frac{H_i}{\nu_i-\nu_j}\right), \tag{8}$$

where

$$\Delta\phi_m(\nu_j)=-0.28g_m \sin\left(\frac{\nu_m-\nu}{0.3\Delta\nu_m}\right) \tag{9}$$

for the line shape given by Eq. (7). Here $g_m$ is the maximum value of the fractional energy gain per pass, $\Delta\nu_c$ is the width of the cavity resonance, $\Delta\nu_m$ is the width of the Doppler broadened line, and $f$ is the fractional energy loss per pass. The second term on the right would be applicable to oscillation in only one axial mode, and for $\nu_m-\nu$ small, and $g_m\approx f$ reduces to the result for the pulling effect in a maser,[24] which is given by

$$\nu-\nu_c=(\Delta\nu_c/\Delta\nu_m)(\nu_m-\nu_c). \tag{10}$$

The third term on the right of Eq. (8) is due to the inhomogeneous broadening of the neon laser transition, since a number of axial modes spaced in frequency by $\Delta\nu=c/2d$ can oscillate simultaneously within the Doppler linewidth.[25] This gives the hole repulsion effect where $H_i$ is the width of the hole produced in the line by the $i$th cavity resonance. Frequency shifts due to these hole repulsion effects may be as large as those due to homogeneous broadening, and for a number of simultaneous laser oscillations in axial modes such effects become quite complicated.

Although such hole repulsion effects can occur within the separate lines corresponding to the circular polarized

[24] J. P. Gordon, H. J. Zeiger, and C. H. Townes, Phys. Rev. **99**, 1264 (1955).

[25] This term only holds for $H_i<(\nu_i-\nu_j)$ and is not valid for a symmetric placement of an odd number of holes in a stationary cavity because of overlapping "mirror image" holes. Expressions valid in this limit were given by W. R. Bennett, Jr., in the Third International Symposium on Quantum Electronics, Paris, France, 1963 (unpublished).

transitions, we shall neglect them in discussing the frequency splitting due to magnetic fields. This is because such effects are quite complicated and not fully understood, and also because they can be reduced by operating close to threshold, or eliminated by using shorter lasers so that the axial mode spacing is increased. With $\Delta\nu_c/f=c/2\pi d$ equal to $0.382\times10^8$ sec$^{-1}$, where $d=125$ cm for our laser, a Doppler linewidth of 800 Mc/sec and a $g$ value of 1.3 for upper and lower states, we obtain from Eq. (8) a value of the low-frequency splitting of an axial resonance given by

$$\nu_B\approx1.62g_mH\times10^5 \text{ cps} \tag{11}$$

for small values of $\nu_m-\nu$. Thus with an axial field of 30 Oe, beat frequencies of 100 kc/sec should be observed for $g_m=2\%$. In practice the observed beat frequencies are of this order, a typical value being 65 kc/sec for a magnetic field of 36 Oe. These depend somewhat on the reflector alignment and on the presence of other axial modes.

We have so far considered only an axial magnetic field, but similar considerations apply for the transverse field case shown in Fig. 5. In this case all transitions $\Delta m=0, \pm1$ occur. Three separate lines are now available corresponding to the $\sigma_+$, $\sigma_-$, and $\pi$ transitions, and a given axial resonance can now split into three oscillations linearly polarized in orthogonal directions. All such beats arise from laser oscillations with orthogonal polarizations, and in order to detect them with a photomultiplier, a Nicol prism or other analyzer must be inserted into the laser beam. As indicated in Fig. 4 the 120 Mc/sec beats arise from different axial modes which will also undergo a splitting in the magnetic field. Such a splitting must be distinguished from that due to the pulling and repulsion effects relevant to the degenerate case.[23] The polarizations of the axial modes may be circularly or linearly polarized in the same or in orthogonal directions, and can be analyzed by rotating the Nicol prism. Such orthogonal transitions are also important in any explanation of how simultaneous oscillations on a $TEM_{00q}$ and associated $TEM_{10q}$ mode, giving the familiar 1 Mc/sec beat, can occur within the same natural linewidth. So far as we can ascertain such beats arise from modes with orthogonal polarizations, and are extremely difficult to observe unless an analyzer is inserted into the laser output beam.

The region in Fig. 4 over which the circularly polarized transitions overlap is important in discussing the effect on the confocal laser of an applied axial magnetic field. Such a laser has a built in analyzer due to the Brewster angle windows, and produces a linearly polarized output. For axial magnetic fields such that the Zeeman levels do not overlap, the transitions within the discharge are still circularly polarized, and are induced to emit coherently by the oppositely rotating circular polarized waves into which the linearly polarized output may be resolved. For very high gains per pass it is possible for oscillation to occur using only one of the circularly polarized transitions, but in general for transitions such as the He—Ne 1.153$\mu$ line, photons of both types must be used with the transitions $\Delta m=\pm1$ induced in phase, so that they may be combined to give the required linear polarization with sufficient gain per pass. Such a process can only occur within the overlap region of the gain curves for opposite circular polarizations, and consequently an increasing axial magnetic field applied to the confocal laser will gradually inhibit oscillation. As indicated by Eq. (2) interference effects will occur at values of magnetic field such that the states overlap which may also lead to variations in the intensity of the laser oscillation. Photons from both of the right- and left-handed circularly polarized transitions must thus be combined to sustain the oscillation when an axial magnetic field is applied to the confocal laser, and the low-frequency beats do not arise in this case, although they may be present when a transverse magnetic field is applied and the Brewster window is orientated to pass the $\sigma$ transitions.

The detailed analysis by Lamb[26] of the degenerate case, which takes into account the velocity distribution of the atoms and the coupling effects between axial modes, is also important for investigations of the Zeeman effect. Some results presently described are that atoms of both positive and negative velocities in the distribution must take part in a given axial resonance,[27] and thus two holes, symmetrical about the center, are made in the Doppler broadened line as shown in Fig. 5. A dip in the power output when a single axial resonance is tuned to the line center is predicted, together with coupling between axial modes and frequency locking effects, when modes become symmetrial about the line center. Similar considerations apply for the Zeeman effect, particularly when simultaneous oscillations occur in a number of axial modes. These, however, will not affect the general conclusions on the polarization, the low-frequency splitting of an axial resonance, or the possibility of coherence effects at low values of magnetic fields. The complicated effects due to this coupling between axial modes indicates that some measurements and the theoretical interpretation would be simplified by using a single resonance at the center of the Doppler distribution. Further observations can ensure this by employing shorter lasers utilizing if necessary the higher gain transitions now available.[27,28]

---

[26] W. E. Lamb, Jr., Third International Symposium on Quantum Electronics, Paris, France, 1963 (unpublished). See also R. A. McFarlane, W. R. Bennett, Jr., and W. E. Lamb, Jr., Phys. Rev. Letters **10**, 189 (1963).

[27] W. R. Bennett, Jr., Suppl. Appl. Opt. **1**, 24 (1962).

[28] C. K. N. Patel, W. L. Faust, and R. A. McFarlane, Appl. Phys. Letters **1**, 84 (1962).

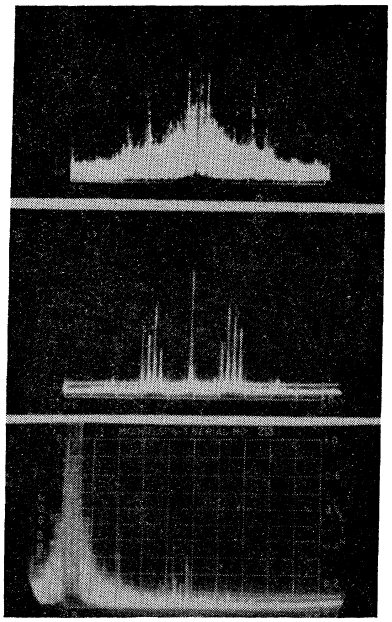

FIG. 6. Upper trace—noisy low-frequency beats due to stray transverse magnetic field of 4 Oe. Frequency sweep ±200 kc/sec. Middle trace—strong low-frequency beat phenomena between oppositely circularly polarized modes. Axial magnetic field 30 Oe, frequency sweep 50 kc/sec/cm. Lower trace—strong low-frequency beats and 1 Mc/sec beats between axial and transverse modes. Axial magnetic field 45 Oe. Frequency sweep 2 Mc/sec.

### 3. EXPERIMENTAL RESULTS

#### a. Planar Laser

The He—Ne laser operated on the 1.153$\mu$ transition and was of the planar or internal optics type. Our initial reflectors were flat to $\lambda/100$ and were spaced 125 cm apart, giving an axial mode separation of 120 Mc/sec. These reflectors gave very clean low-frequency beat spectra, and laser oscillations occurred in a single normal mode of the resonator, there being a bias towards operation in the $TEM_{10q}$ mode. Later these reflectors were damaged by a break in the vacuum system and new ones were inserted. Although these were flat to $\lambda/200$ they did not give beat-frequency spectra as clean as the original set, and such variations between reflectors have been apparent throughout our observations. The frequencies present in the laser output were analyzed with a photomultiplier detector and spectrum analyzer.

The upper trace of Fig. 6, in which zero frequency is at the center and the sweep is ±200 kc/sec, shows the noisy and erratic low-frequency beats initially observed. On investigation a stray magnetic field of some 4 Oe and transverse to the laser axis was found. This figure should be compared with Fig. 1 of Ref. 13 in which the 1 Mc/sec beats between an axial mode and its associated $TEM_{10q}$ mode are also shown. While the polarization of these initial low-frequency beats was erratic, the 1 Mc/sec beats were always due to modes with orthogonal linear polarizations, and were not readily seen unless a Nicol prism was inserted into the beam. Such polarization studies are easily made by observing the variation in the beat-frequency pattern on rotating the analyzer, particularly for 120 Mc/sec beats between axial modes.

Figure 6—middle trace—shows the effect of applying a magnetic field of some 30 Oe along the axis of the laser when operating well above threshold. Here the frequency sweep is ±50 kc/sec/cm, and the low-frequency beat spectra is very evident, the gain of the spectrum analyzer having been reduced by 20 dB, as evident by the greatly reduced noise level. All these beats arise from modes of opposite circular polarization and disappear when the analyzer is removed from the laser beam. The pronounced regular spacing between the beats is indicative of the occurrence of some relaxation or modulation phenomena, and similar results obtained with other reflectors are given later. The frequency interval between the beats of some 3–10 kc/sec varied with reflector adjustment, and such patterns were observed for the $TEM_{00q}$ and $TEM_{10q}$ modes, and for other mode patterns as seen on the image converter. As the rf excitation level was increased from threshold values the number of such frequency components increased from one or two to around twenty, the frequency spacing for a given reflector adjustment remaining approximately the same. The lower trace of Fig. 6 which has zero frequency on the left-hand side, and a frequency sweep of 2 Mc/sec, shows the large number of low-frequency beats and also the increased number of beats around 1 Mc/sec between the axial and associated off-axis or $TEM_{mnq}$ modes, which were obtained with a new set of plane reflectors. Such complicated patterns are typical of the limited number of high-quality reflectors, flat to $\lambda/200$, which we have used so far. Beat-frequency patterns are dependent on the mode content or reflector adjustment, and less complicated beat patterns can be

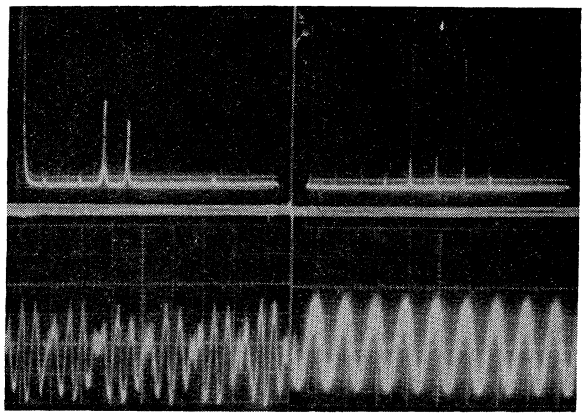

FIG. 7. Low-frequency beats and modulation waveforms. Right traces—transverse magnetic field 40 Oe; frequency sweep 50 kc/sec/cm; time sweep 20$\mu$ sec/cm. Left traces—transverse magnetic field 25 Oe; frequency sweep 50 kc/sec/cm; time sweep 100$\mu$ sec/cm.

obtained. Questions of threshold and possibly coupling between normal modes of the planar resonator are important here. Of interest is that the first set of reflectors flat to $\lambda/100$, with the coating techniques then used, gave the simplest beat patterns. However, all such beats arise from modes with orthogonal circular polarizations.

Figure 7 shows some striking low-frequency beats together with the respective modulation waveforms in the time domain. A magnetic field of 40 Oe and transverse to the laser axis was used in the right-hand traces, the frequency sweep being 50 kc/sec/cm and the time sweep $\mu$sec/cm. Similarly, for the left-hand traces the frequency sweep was the same, the time sweep was 100 $\mu$sec/cm, and the transverse field was 25 Oe. These patterns were obtained with appropriate reflector adjustments for the single and double beat, and with an analyzer at 45° orientation, since the polarizations are now linear and orthogonal for transverse magnetic fields. The origin of the double low-frequency beat for a transverse magnetic field was discussed in the previous section, and depends also on the reflector adjustment.

Beat frequencies between $TEM_{00q}$ modes and $TEM_{10q}$ modes at frequencies of 119, 120, and 121 Mc/sec are shown in Fig. 8, taken with the stray magnetic field of 4 Oe transverse to the laser axis. Since the 120 Mc/sec frequency separation between such modes is greater than the natural linewidth of the laser transitions, such modes of oscillation can be linearly polarized in the same or in orthogonal directions. The upper trace with the analyzer in the vertical plane shows that the left-hand beat is due to modes with orthogonal polarizations. The center trace taken with the polarizer at 45° shows all three beats. The lower trace with the polarizer at 90° to the vertical shows that the beats at 119 and 121 Mc/sec have one component polarized in the vertical plane. The middle trace shows that a weak beat with orthogonal polarizations is present in all three frequencies. The stronger of the two beats at 120 Mc/sec showed a third type of angular dependence, being a maximum at 0° and 90° orientation and a minimum or zero at 45°. Reasons for this may be the degeneracy of the Zeeman levels at this low field, or the beat consists of a number of unresolved beats from other axial modes. A hybrid type of mode pattern was observed on the image converter when such beats were present. Similar beats occur when axial magnetic fields are applied, and at fields around 30 Oe all such modes are circularly polarized.

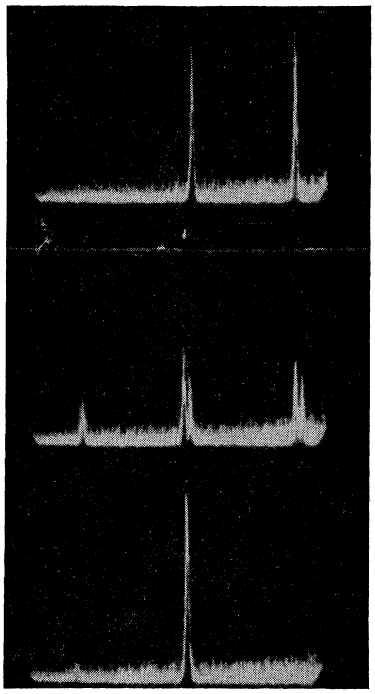

FIG. 8. Effect of polarizer on the 119 (left), 120, and 121 Mc/sec (right) beats between axial and higher *TEM mnq* modes of the planar He–Ne laser. Upper—polarizer at 0°; middle—polarizer at 45°; lower—polarizer at 90° to vertical. Modes linearly polarized; stray transverse magnetic field at 4 Oe is present.

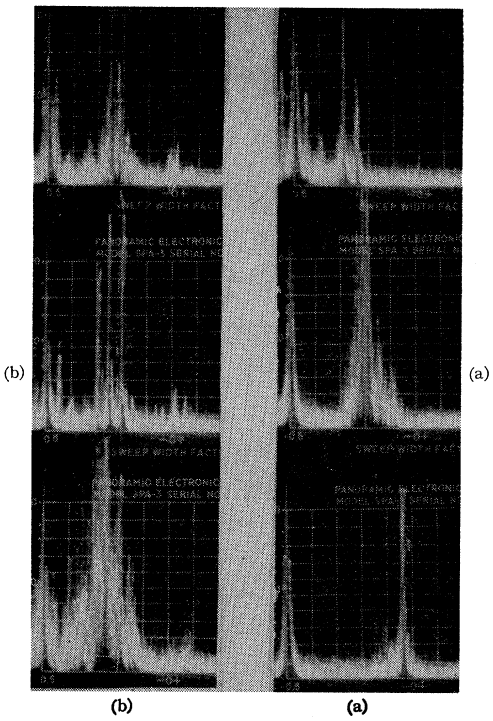


FIG. 9. (a) Multiplicity of low-frequency beats and Zeeman tuning of the planar laser. Axial magnetic field—upper trace 31 Oe; middle trace 40 Oe; lower trace 55 Oe. (b) Low-frequency beats and relaxation phenomena. Axial magnetic field—upper trace 28 Oe; middle trace 31 Oe; lower trace 34 Oe. All modes oppositely circular polarized; frequency sweep 20 kc/sec/cm.

Figure 9(a) shows the increased multiplicity of low-frequency beats taken with a later set of reflectors, and should be compared with Figs. 6 and 7 taken with our original set. Here the beats are many and varied, but occur in a similar frequency range 20–100 kc/sec depending on the magnetic field which is 31, 40, and 55 Oe for the three traces. Zero frequency is on the

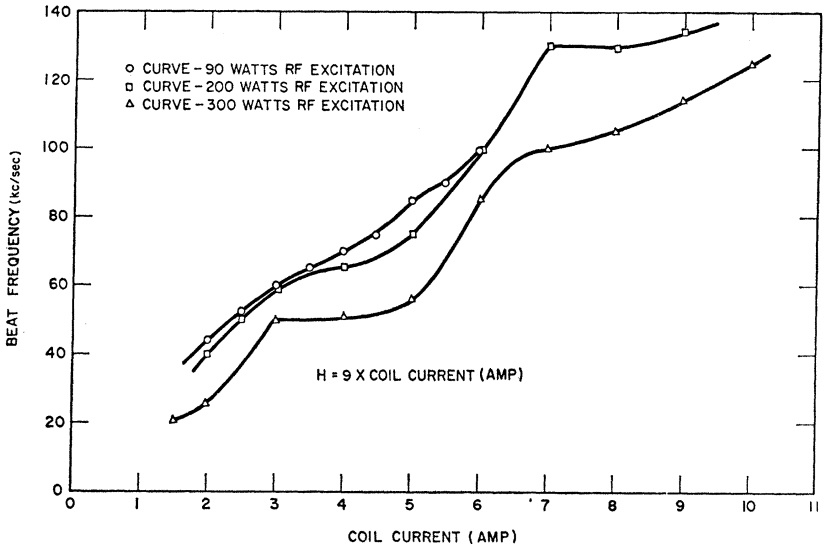


FIG. 10. Planar He—Ne laser—variation of the low-frequency Zeeman splitting of axial resonances with magnetic field and rf excitation level. (rf frequency 29 Mc/sec.)

left-hand side, and the frequency sweep is 20 kc/sec/cm. The effect of Zeeman tuning of the laser is clearly shown by the shift to the right of the beat frequencies with increasing magnetic field. Some cleaning up of the beat-frequency pattern is evident at the lower and higher values of magnetic field. All such beats are due to modes of opposite circular polarization and disappear at values of magnetic field above some 100 Oe, when the Doppler broadened Zeeman transitions separate beyond threshold for simultaneous oscillations at a given axial mode in both circular polarizations. Figure 9(b) shows that the relaxation or modulation phenomena, corresponding to that shown in Fig. 6 for our original reflectors, persists for the new set. The values of magnetic field are 29, 31, and 34 Oe, and indicate that such a phenomenon depends fairly sharply on the magnetic field. The middle trace shows the closest approach to a regular spaced pattern, and the fact that the beats are obviously present above and below this value of magnetic field appears to rule out the possibility of threshold effects, unless another axial mode takes over. It is significant that at a magnetic field of 31 Oe, the Zeeman separation of the lines given by $2.8gH$ Mc/sec is 113 Mc/sec, which approximates the separation between axial modes of our Fabry-Perot resonator.

The fine tuning of the laser by the Zeeman effect is shown in Fig. 10 for various relative levels of rf excitation. At low values of rf excitation, or gain, the curve is reasonably linear as indicated by Eq. (11). The curve does not pass through the origin, and in fact the low-frequency beats become very erratic at values of magnetic field below 15 Oe, and finally disappear, in general accordance with the noise like character of the beats exemplified in the upper trace of Fig. 6 for the stray field of 4 Oe. The slope of the curve at the lowest value of rf excitation is 1.4 kc/sec/Oe in reasonable agreement with the value 1.6 kc/sec/Oe deduced from Eq. (11) with $g_m=1\%$. Also the beat frequency for a magnetic field of 54 Oe is 90 kc/sec in reasonable agreement with the value 100 kc/sec deduced from Eq. (11). For the higher values of rf excitation, or gain per pass, the agreement is not as good. The beat frequency for a given value of $H$ decreases with increasing gain, and the slope is approximately the same

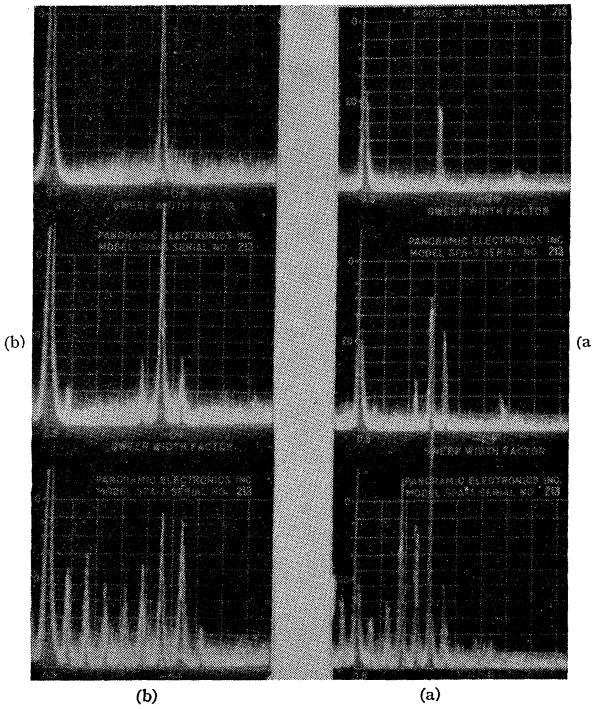


FIG. 11. (a) Variation of frequencies in relaxation phenomena with rf excitation power. Upper trace—150 W; middle—220 W; lower—300 W (relative values). Axial magnetic field 31 Oe; frequency sweep 20 kc/sec/cm. (b) Axial magnetic field on laser. Upper trace—low-frequency splitting due to dc field. Middle and lower traces—modulation due to increasing amplitude of ac magnetic field of frequency 8 kc/sec.

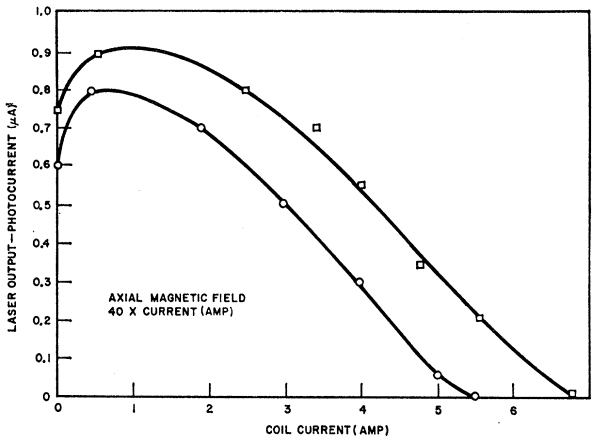


FIG. 12. Confocal He—Ne laser—variation of output power with axial dc magnetic field. Upper curve is for a higher level of rf excitation.

as for smaller values of gain. These effects are presumably due to the increased number of axial modes at the higher values of gain, and the consequent appearance of hole repulsion effects which were neglected in deducing Eq. (11). The appearance of bumps on the curves for the higher values of gain is also due to the increased number of simultaneously oscillating axial modes. It is interesting that the magnetic field interval of some 36 Oe between the bumps remains fairly constant with gain variation, and for upper and lower state $g$ values of 1.3 corresponds a Zeeman splitting of some 120 Mc/sec which again is the separation of the axial resonances of our laser cavity.

Figure 11(a) shows the variation with rf power level of the beats, or frequency components, of the relaxation phenomena discussed in Fig. 9(b). An axial magnetic field of 31 Oe is present, and the relative levels of rf excitation are 150, 220, and 300 W from the top to the bottom traces. The gradual increase in the number of frequency components spaced some 12 kc/sec apart is evident. Figure 11(b) shows the effect of applying an ac axial magnetic field of frequency 8 kc/sec together with a dc or biasing axial magnetic field. The top trace shows the low-frequency beat with no ac magnetic field, while the middle and bottom traces show the effect of an increasing amplitude of the ac magnetic field. The bottom trace exemplifies a frequency modulation of the laser, and should be compared with Fig. 11(a) where similar effects are in evidence.

### b. Confocal Type Laser

This design utilizes a gas-filled tube with Brewster angle windows inside the resonator, which may be of the highly degenerate confocal type, or of the spherical type. For a spherical resonator the eigenvalues and eigenfunctions are the complex conjugates of those for the planar resonator, and the modal patterns of the resonator are considerably simplified, while maintaining the relative ease of adjustment as compared with the planar-type resonator. However, the changes in polarization due to Zeeman effects are not as readily observed, since the polarization must remain linear and in the plane of incidence of the Brewster angle windows. The experimental results given here were obtained with a confocal type resonator, but are also applicable to the spherical or other nonconfocal type resonator.

Figure 12 shows the effect of applying a steadily increasing axial dc magnetic field to the confocal laser.[29] The upper of the two curves corresponds to a somewhat higher level of rf excitation than the lower curve. After a turning over region the power output decreases to zero at fields in excess of some 200 Oe, due to the gradual reduction in the overlap region of the circularly polarized transitions as the axial magnetic field increases, which was discussed in Sec. 2. The turnover region at magnetic fields around 30 Oe is interesting and must again be associated with interference or coherence effects between the various Zeeman transitions at low values of magnetic field. The separation of the sublevels is given by $\Delta\nu = gH \times 1.4$ Mc/sec, and for $H = 30$ Oe, and $g = 1.3$ this gives $\Delta\nu = 55$ Mc/sec which agrees approximately with the expected linewidths of the Zeeman levels. Further experimental and theoretical interpretation of the effect is required, but present results agree with the expected phenomena. Any stray magnetic fields are well below the relatively high value of 30 Oe at which the effect occurs. The shift of the curve for the higher level of rf excitation is also explained since the linewidths for induced emission will be broadened at higher field intensities in the laser. Amplitude modulation of the laser has been obtained by applying an ac axial magnetic field and biasing the laser to the relatively linear region by a dc axial magnetic field. Without the bias the laser is modulated at twice the modulating frequency since the Zeeman levels cross over. Modulation rates depend on the time constant of the laser cavity, and on the precession rates of the atoms in the dc magnetic field. The method appears suitable for the determination of precession rates by applying ac fields of varying frequency to the

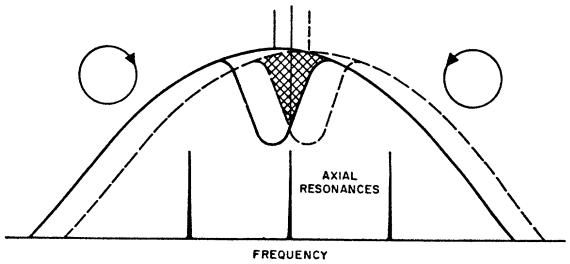


FIG. 13. Weak axial magnetic field—overlapping of states and depolarization effects.

[29] This data was reported by the authors at the Third International Symposium on Quantum Electronics, Paris, France, 1963 (unpublished). Similar results have also been obtained by R. G. Buser, J. Kainz, and J. Sullivan, Appl. Opt. 2, 861 (1963).

laser in an analogous way to those used by Fermi and Rasetti,[20] to study the depolarization of the resonance radiation of mercury.

## 4. PERTURBATION TREATMENT OF COHERENCE

In contrast to the spontaneous emission processes used to consider depolarization effects in resonance radiation studies, similar effects in the laser must consider the induced emission due to the relatively intense and highly monochromatic radiation involved. The polarizations of the modes of oscillation in zero magnetic field are linear and orthogonal with orientations which appear to depend on anisotropies in the reflecting films. When the Zeeman levels are shifted beyond their natural linewidth, which is the same for all sublevels corresponding to the same $J$ value, the specific Zeeman polarizations, such as circular with an axial magnetic field, are observed. As the magnetic field is reduced the sublevels overlap, the various induced transitions become coherent, and polarization changes occur which degenerate into the polarization observed in zero magnetic field. By the principle of spectroscopic stability this polarization is fixed, but the manner in which it is approached will depend on the location of the particular axial resonance with respect to the Doppler broadened transitions. Figure 13 shows this for the symmetrical situation, from which it is clear that the axial resonance can now induce coherent transitions between the Zeeman sublevels comprising the state vector of an atom. Thus, the polarization changes involved as the magnetic field is reduced to zero will depend on the location of the axial resonance with respect to the natural linewidths shown in Fig. 13, and changes from circular to elliptical and linear polarizations may be expected.

Consider first the case of two states $a$ and $b$ with damping constants $\gamma_a$ and $\gamma_b$, and an applied electric dipole perturbation $\mathcal{H}'(t)$. Schrödinger's equation may be written

$$i\hbar\partial\psi/\partial t=[\mathcal{H}_0+\mathcal{H}'(t)]\psi, \tag{12}$$

and the state vector of the atom expressed as

$$\psi(\mathbf{r},t)=a(t)u_a(\mathbf{r})e^{-iE_at/\hbar}+b(t)u_b(\mathbf{r})e^{-iE_bt/\hbar}, \tag{13}$$

where $a(t)$ and $b(t)$ are the time-dependent probability amplitudes. From Eqs. (12) and (13) and the relations $\mathcal{H}_0u_a=E_au_a$, etc., we obtain the equations

$$\begin{aligned} i\hbar\dot{a}&=H_{ab}e^{-i(\omega-\omega_{ab})t}b-i\hbar(\gamma_a/2)a,\\ i\hbar\dot{b}&=H_{ba}e^{i(\omega-\omega_{ab})t}a-i\hbar(\gamma_b/2)b, \end{aligned} \tag{14}$$

where $H_{ba}=e(E_0/2)(b|\mathbf{e}_\lambda\cdot\mathbf{r}|a)$, etc., $\omega_{ab}=(E_a-E_b)/\hbar$, $eE_0\cos\omega t$ is the perturbation with polarization $\mathbf{e}_\lambda$, and the rotating wave approximation is used. The decay constants $\gamma$ have been introduced in a phenomenological way, but as pointed out by Lamb[31] this can be justified by a quantum mechanical argument. Supposing $a(0)=1$ and $b(0)=0$, the quantity $|b(t)|^2$ is the probability that the atom is in state $b$ at time $t$, and that a photon of type $\mathbf{e}_\lambda$ has been emitted. Steady-state conditions will depend on the particular application, for the laser where $\gamma_b>\gamma_a$, the total probability that the atom has decayed by stimulated emission may be written as

$$P_s=\gamma_b\int_0^\infty|b(t)|^2dt, \tag{15}$$

and hence using Eqs. (14) it is found that[23]

$$P_s=\frac{\gamma_b(\gamma_a+\gamma_b)|2H_{ab}/\hbar|^2}{4(\omega-\omega_{ab})^2\gamma_a\gamma_b+(\gamma_a\gamma_b+|2H_{ab}/\hbar|^2)(\gamma_a+\gamma_b)^2}. \tag{16}$$

A similar result may be deduced by setting up a density matrix for the steady-state populations,[31] and thus avoiding the consideration of transient effects. The line is thus Lorentzian in shape, centered at $\omega=\omega_{ab}$, and with a width at half-height of

$$\Delta\omega=(\gamma_a+\gamma_b)[1+|2H_{ab}/\hbar|^2/(\gamma_a\gamma_b)]^{1/2}. \tag{17}$$

The transition probability thus depends on the difference in frequency $\omega-\omega_{ab}$ between that of the line center and of the inducing radiation, and is symmetrical in this factor.

Equations (14) may be generalized to a set of $N$ levels comprising the Zeeman sublevels $\mu$ and $m$ of the upper and lower states respectively, with the result that

$$i\hbar\dot{a}_j=\sum_{k=1}^{N}\left(H_{jk}e^{i\omega_{jk}}-\frac{i}{2}\hbar\gamma_k\delta_{jk}\right)a_k \tag{18}$$

with $H_{jj}=0$, $j=1,\ 2\cdots,\ N$, and $H_{jk}=(j|\mathcal{H}'(t)|k)$. Here in addition to electric dipole transitions between the sublevels of the states $a$ and $b$, we may have magnetic dipole transitions between the Zeeman levels of $a$ or $b$ due to applied rf fields at the Larmor frequency. With appropriate matrix elements $H_{jk}=e(j|\mathbf{E}(t)\cdot\mathbf{r}|k)$ for electric dipole transitions and $H_{jk}=\gamma_g(j|\mathbf{J}\cdot\mathbf{H}(t)|k)$ for the rf perturbation, Eq. (17) is applicable to double resonance experiments on the gas laser.

Equation (18) will be applied to the resonance line of mercury with no hyperfine structure effects, and without any rf perturbation between the Zeeman levels. This will serve to illustrate the effect when the Zeeman levels are such that $geH/2mc<1/\tau$ and coherence occurs between the various transitions. The resonance line of mercury has a nondegenerate lower state $|g\rangle$ $(j=0)$, and a triply degenerate upper state $|1\rangle$, $|0\rangle$, and $|-1\rangle$ with $j=1$. For the symmetrical case shown in Fig. 13 the equations become

$$\begin{aligned} i\hbar\dot{a}_j&=b_0e^{i(\omega_{jg}-\omega)t}H_{jg}-i\hbar\gamma_ja_j/2, \quad j=1,0,-1,\\ i\hbar\dot{b}_0&=\textstyle\sum_j a_je^{-i(\omega_{jg}-\omega)t}H_{gj}, \end{aligned} \tag{19}$$

where $b_0$ is the probability amplitude of the ground state $|g\rangle$, $\omega_{1g}-\omega=\omega-\omega_{-1g}=geH/2mc$, and $\omega$ is the

[30] E. Fermi and F. Rasetti, Z. Physik **33**, 246 (1925).

[31] W. E. Lamb, Jr., and T. M. Sanders, Jr., Phys. Rev. **119**, 1901 (1960); L. R. Wilcox and W. E. Lamb, Jr., Phys. Rev. **119**, 1915 (1960).

angular frequency of the laser oscillation. $H_{gj}$ is the electric dipole matrix element $e(E_0/2)(g|\mathbf{e}_\lambda\cdot\mathbf{r}|j)$, and $\mathbf{e}_\lambda$ is the specific polarization of the laser oscillation. To determine this we must insert the appropriate matrix elements corresponding to allowed transitions $(g|\mathbf{e}_\lambda\cdot\mathbf{r}|j)$, which will determine the probabilities for the emission of a photon of type $\mathbf{e}_\lambda$. All such transitions with their polarizations must be summed in a coherent way to determine the polarization of the oscillation for the appropriate orientation of the magnetic field. For present purposes we consider the situation during the build up of oscillation from spontaneous emission, and take $b_0(0)=0$ and $b_0$ small for a time $t$. Initially the atom is in a mixture of states $|\mu\rangle$ with equal probabilities, and we thus assume $\dot{a}_1=-\gamma a_1/2$, etc. The equation for $b_0$ can then be integrated directly, and for an axial magnetic field along the laser axis, which we take as the $z$ axis, we obtain

$$b_0=\left(\frac{C}{i\hbar}\right)\left[H_{g1}\left(\frac{1-e^{-(i\Omega+\gamma/2)t}}{\gamma/2+i\Omega}\right)+H_{g-1}\left(\frac{1-e^{(i\Omega-\gamma/2)t}}{\gamma/2-i\Omega}\right)\right], \quad (20)$$

where $\Omega=(\omega_{1g}-\omega)$, and $C$ is a constant. The matrix elements $H_{g1}$, $H_{g-1}$ correspond to $\mathbf{e}_\lambda$ being left- and right-handed circularly polarized respectively, and the product terms $H_{g1}H_{g-1}^*$ involved in $|b_0(t)|^2$, and pertaining to one type of polarization $\mathbf{e}_\lambda$ thus vanish. Then since the moduli of the coefficients of $H_{g1}$ and $H_{g-1}$ are equal, we have equal probabilities for left- and right-handed circularly polarized photons, which combine coherently to give a linearly polarized output. This can also be seen by using the complex representation of circularly polarized waves, corresponding to the matrix elements $H_{g1}$ and $H_{g-1}$; we then find the resultant polarization is determined by

$$(\mathbf{i}+i\mathbf{j})\left(\frac{1-e^{-(i\Omega+\gamma/2)t}}{\gamma/2+i\Omega}\right)-(\mathbf{i}-i\mathbf{j})\left(\frac{1-e^{(i\Omega-\gamma/2)t}}{\gamma/2-i\Omega}\right), \quad (21)$$

hence the real part of this expression is zero, and the radiation is linearly polarized at some angle to the $x$ direction. Equation (20) is analogous to the Breit equation (2) discussed in Sec. 2.

The interesting result emerges that for the symmetrical case, where $\omega_{1g}-\omega=\omega-\omega_{-1g}$, the radiation will remain linearly polarized within the natural linewidths as the magnetic field increases from zero. When the field is such that $geH/mc>1/\tau$ the coherence breaks down and oscillations occur with the normal circular polarizations of the Zeeman transitions, and low-frequency beats due to the splitting of axial modes occur. When the axial resonance or laser frequency is asymmetrical with respect to the natural linewidths shown in Fig. 13, the polarization will become elliptical since the circular polarized transitions then have unequal transition probabilities, and combine coherently to give elliptical polarization. Such results may also be deduced from Eq. (16) using the symmetry of the line shape of $P_s$, the transition probability for a photon of type $\mathbf{e}_\lambda$. Results applicable to any other orientation of magnetic field can be obtained in a similar way. Although the actual laser transition occurs between excited states, each with its decay constant and Zeeman sublevels, similar results will be obtained in this more complicated case. A higher number of transitions is involved and the $g$ factors of both levels must be considered. While we have considered a single axial resonance, the same considerations apply for other simultaneously oscillating axial modes, and beats will be obtained between such modes linearly polarized in the same and in orthogonal directions. When the axial resonance is not symmetrical with respect to the Doppler distribution the polarizations will be elliptical, and the use of such magnetic fields should permit the resonance to be centered on the line. In view of the ideal axial symmetry of the planar laser, the orientation of the polarizations would be different each time the oscillations were initiated. In practice this does not occur due to anisotropies in the reflecting layers, or to other perturbations in the system, which favor photons with a given polarization. Once this occurs the polarizations in zero magnetic field, according to principle of spectroscopic stability, should correspond to those obtained by having a strong magnetic field along this direction of polarization.

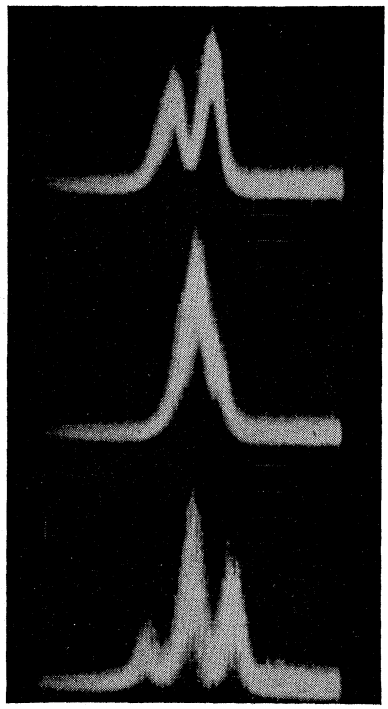

FIG. 14. Axial magnetic field—de-polarization effects in He—Ne laser. Upper—zero field, modes linearly polarized at +60° and −30° to vertical. Middle—magnetic field 14 Oe, polarizations still essentially linear. Lower—magnetic field 27 Oe—modes circularly polarized.

Figure 14 shows the beat frequencies at 120 Mc/sec between simultaneously oscillating axial modes of the laser in the presence of an increasing axial magnetic field. As mentioned earlier the axial mode beats must be used for these investigations, since the low-frequency beats become very erratic and tend to disappear at low values of magnetic field due to the coherence which occurs between the states. The upper trace, with no solenoid current, shows axial beats due to linearly polarized modes at $+60°$ and $-30°$ to the vertical. The splitting of these 120 Mc/sec beats of some 50 kc/sec is due to frequency pulling and coupling effects in the medium. The polarizations of these modes are thus linear and orthogonal, and an analyzer must be used in the output beam. A residual magnetic field of one or two oersted was present along the axis of the laser when the solenoid current was zero. The middle trace in which the axial field is 14 Oe, shows that some change in the mode splitting has occurred, but the polarizations of the oscillations are still essentially linear, even at this relatively high value of magnetic field. In the lower trace the axial magnetic field is 27 Oe and the polarizations of the modes comprising the beats are all circular. The outer components originate from appositely rotating circularly polarized modes, and the center one from modes rotating in the same direction. At other times elliptical polarization has been observed, such effects occurring with almost any mode of oscillation of the resonator as seen on the image converter. Similar results have been obtained with transverse magnetic fields, when the polarizations seen are mainly linear and orthogonal at all values of magnetic field, but orientated at arbitrary angles as above, which are apparently dependent on reflector characteristics.

## 5. CONCLUSIONS

The observed Zeeman effects in general explain the specific polarizations which occur in planar lasers, and are also important in discussing the various beat phenomena. For isotropic reflectors, the polarizations will be determined by the orientation of the magnetic field, and for transverse and axial magnetic fields, of values such that the Zeeman sublevels do not overlap, these will be linear or circular and orthogonal. Anisotropy in the reflecting films may well lead to variations in these specific orientations of the polarizations, and departures also occur when the Zeeman levels overlap due to coherence between the induced transitions. Thus, with an axial magnetic field the polarization will remain linear in the symmetrical case until the Zeeman levels separate. For an asymmetric location of the axial resonance with respect to the line, elliptical polarization should be observed. For higher values of magnetic fields, the states separate and low-frequency beats occur due to a splitting of an axial resonance, these are always polarized in orthogonal directions, and represent a method for the study of anomalous dispersion effects in the gas medium.

By utilizing the shorter lasers possible with the higher gain transitions, the complexities of mode coupling effects in the media will be avoided, and the application of more uniform and higher magnetic fields made possible. In this way the polarization changes of a single mode may be measured and used to study linewidths of the laser transition. Variations of this due to variations in laser output power and gas pressure can thus be investigated. The single resonance can be set on the center of the line either by using the Lamb dip, or by further investigation of the linear polarization obtained within the natural linewidth with axial magnetic fields when the resonance is centered. Accurate determinations of $g$ factors can thus be made.

As already indicated Eq. (18) can be applied to double resonance studies, utilizing the induced emission from a single or a number of oscillating axial modes, when coherence is imparted to the Zeeman sublevels by an additional rf perturbation at the Larmor frequency. Such studies are of potential importance for linewidth measurements, and for the internal modulation of the laser. Finally, there are indications that coupling effects between resonances are occurring at magnetic fields around 30 Oe when the transitions $\Delta m = \pm 1$ are separated by some 120 Mc/sec which is the separation between axial modes in our laser. These may be due to the effects of "mirror image" holes[27] and associated frequency locking phenomena within the Doppler linewidths.

## ACKNOWLEDGMENTS

We express our appreciation of the valuable efforts of W. Proskauer on the construction of the lasers, and those of F. O. Lopex and D. Jacques on instrumentation and measurements.

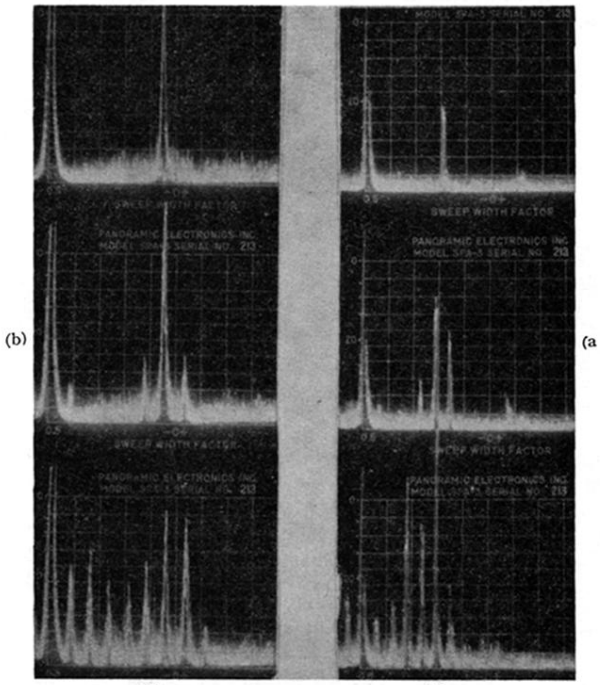


FIG. 11. (a) Variation of frequencies in relaxation phenomena with rf excitation power. Upper trace—150 W; middle—220 W; lower—300 W (relative values). Axial magnetic field 31 Oe; frequency sweep 20 kc/sec/cm. (b) Axial magnetic field on laser. Upper trace—low-frequency splitting due to dc field. Middle and lower traces—modulation due to increasing amplitude of ac magnetic field of frequency 8 kc/sec.

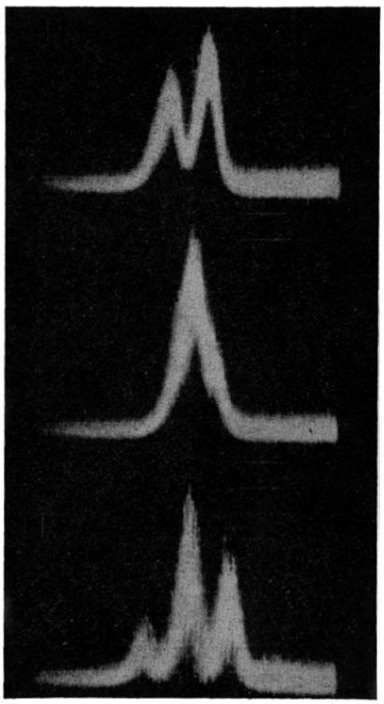

FIG. 14. Axial magnetic field—de-polarization effects in He—Ne laser. Upper—zero field, modes linearly polarized at +60° and −30° to vertical. Middle—magnetic field 14 Oe, polarizations still essentially linear. Lower—magnetic field 27 Oe—modes circularly polarized.

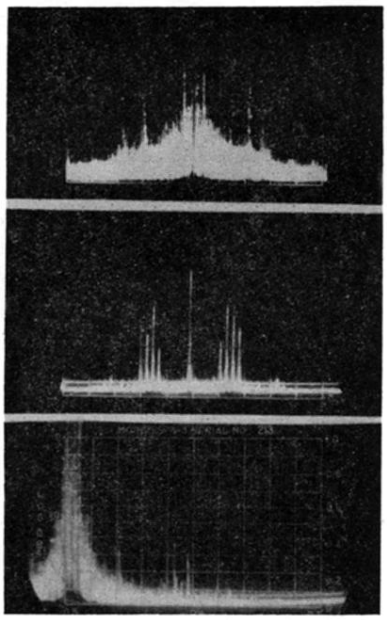

FIG. 6. Upper trace—noisy low-frequency beats due to stray transverse magnetic field of 4 Oe. Frequency sweep ±200 kc/sec. Middle trace—strong low-frequency beat phenomena between oppositely circularly polarized modes. Axial magnetic field 30 Oe, frequency sweep 50 kc/sec/cm. Lower trace—strong low-frequency beats and 1 Mc/sec beats between axial and transverse modes. Axial magnetic field 45 Oe. Frequency sweep 2 Mc/sec.

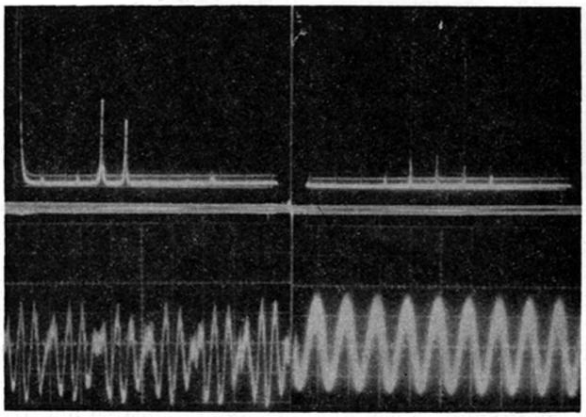

FIG. 7. Low-frequency beats and modulation waveforms. Right traces—transverse magnetic field 40 Oe; frequency sweep 50 kc/sec/cm; time sweep 20 $\mu$ sec/cm. Left traces—transverse magnetic field 25 Oe; frequency sweep 50 kc/sec/cm; time sweep 100 $\mu$ sec/cm.

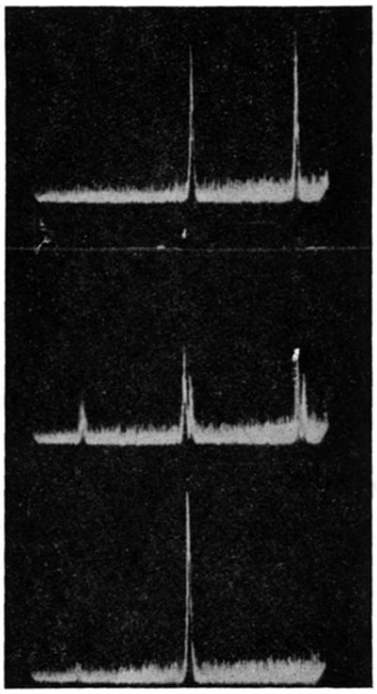

FIG. 8. Effect of polarizer on the 119 (left), 120, and 121 Mc/sec (right) beats between axial and higher *TEM mng* modes of the planar He−Ne laser. Upper—polarizer at 0°; middle—polarizer at 45°; lower—polarizer at 90° to vertical. Modes linearly polarized; stray transverse magnetic field at 4 Oe is present.

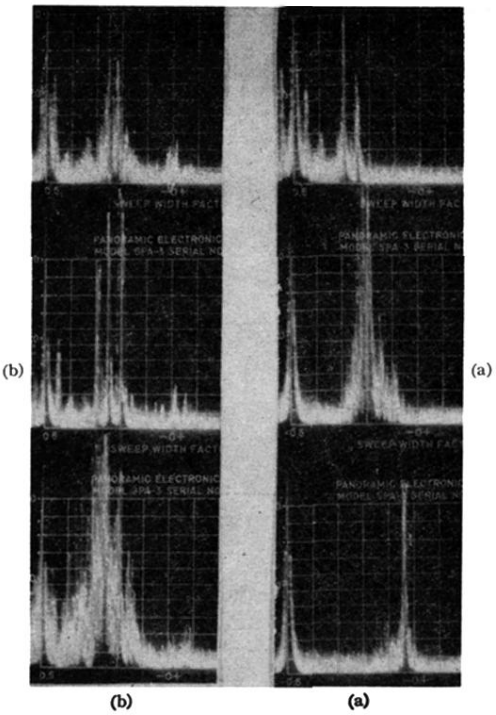


FIG. 9. (a) Multiplicity of low-frequency beats and Zeeman tuning of the planar laser. Axial magnetic field—upper trace 31 Oe; middle trace 40 Oe; lower trace 55 Oe. (b) Low-frequency beats and relaxation phenomena. Axial magnetic field—upper trace 28 Oe; middle trace 31 Oe; lower trace 34 Oe. All modes oppositely circular polarized; frequency sweep 20 kc/sec/cm.